

## Accepted Manuscript

Discovery and Optimization of Novel Piperazines as Potent Inhibitors of Fatty Acid Synthase (FASN)

Matthew W. Martin, David R. Lancia Jr., Hongbin Li, Shawn E.R. Schiller, Angela V. Toms, Zhongguo Wang, Kenneth W. Bair, Jennifer Castro, Shawn Fessler, Deepali Gotur, Stephen E. Hubbs, Goss S. Kauffman, Mark Kershaw, George P. Luke, Crystal McKinnon, Lili Yao, Wei Lu, David S. Millan

PII: S0960-894X(19)30088-5  
DOI: <https://doi.org/10.1016/j.bmcl.2019.02.012>  
Reference: BMCL 26292

To appear in: *Bioorganic & Medicinal Chemistry Letters*

Received Date: 15 January 2019  
Revised Date: 5 February 2019  
Accepted Date: 10 February 2019

Please cite this article as: Martin, M.W., Lancia, D.R. Jr., Li, H., Schiller, S.E.R., Toms, A.V., Wang, Z., Bair, K.W., Castro, J., Fessler, S., Gotur, D., Hubbs, S.E., Kauffman, G.S., Kershaw, M., Luke, G.P., McKinnon, C., Yao, L., Lu, W., Millan, D.S., Discovery and Optimization of Novel Piperazines as Potent Inhibitors of Fatty Acid Synthase (FASN), *Bioorganic & Medicinal Chemistry Letters* (2019), doi: <https://doi.org/10.1016/j.bmcl.2019.02.012>

This is a PDF file of an unedited manuscript that has been accepted for publication. As a service to our customers we are providing this early version of the manuscript. The manuscript will undergo copyediting, typesetting, and review of the resulting proof before it is published in its final form. Please note that during the production process errors may be discovered which could affect the content, and all legal disclaimers that apply to the journal pertain.





## Discovery and Optimization of Novel Piperazines as Potent Inhibitors of Fatty Acid Synthase (FASN)

Matthew W. Martin,<sup>a,\*</sup> David R. Lancia, Jr.,<sup>a</sup> Hongbin Li,<sup>b</sup> Shawn E. R. Schiller,<sup>a</sup> Angela V. Toms,<sup>a</sup> Zhongguo Wang,<sup>a</sup> Kenneth W. Bair,<sup>a</sup> Jennifer Castro,<sup>a</sup> Shawn Fessler,<sup>a</sup> Deepali Gotur,<sup>a</sup> Stephen E. Hubbs,<sup>b</sup> Goss S. Kauffman,<sup>b</sup> Mark Kershaw,<sup>b</sup> George P. Luke,<sup>b</sup> Crystal McKinnon,<sup>a</sup> Lili Yao,<sup>b</sup> Wei Lu,<sup>a,†</sup> and David S. Millan<sup>a,‡</sup>

<sup>a</sup>FORMA Therapeutics, 500 Arsenal Street, Suite 100, Watertown, MA 02472, USA

<sup>b</sup>FORMA Therapeutics, 35 Northeast Industrial Road, Branford, CT 06405, USA

### ARTICLE INFO

#### Article history:

Received

Revised

Accepted

Available online

#### Keywords:

Fatty acid synthase, FASN, de novo lipogenesis, oncology, piperazines

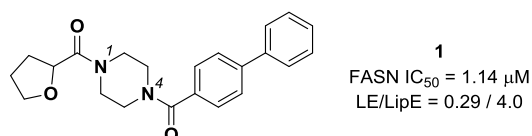
### ABSTRACT

The discovery, structure-activity relationships, and optimization of a novel class of fatty acid synthase (FASN) inhibitors is reported. High throughput screening identified a series of substituted piperazines with structural features that enable interactions with many of the potency-driving regions of the FASN KR domain binding site. Derived from this series was **FT113**, a compound with potent biochemical and cellular activity, which translated into excellent activity in *in vivo* models.

Fatty acid synthase (FASN) is a key enzyme in the de novo lipogenesis (DNL) pathway, catalyzing the synthesis of palmitate and coenzyme A (CoA) from malonyl-CoA and acetyl-CoA. Most normal human tissues preferentially use dietary lipids for synthesis of new structural lipids, and de novo fatty-acid synthesis is usually suppressed, with FASN expression maintained at low levels. By contrast, in cancer cells, the supply of cellular fatty acids is highly dependent on the de novo synthesis with the expression of many of these key enzymes being elevated. As such, FASN is highly expressed in many cancers, including glioblastoma, prostate, ovarian, breast, endometrial, thyroid, colorectal, bladder, lung, thyroid, oral, head and neck, hepatocellular, pancreatic, gastric carcinomas, melanoma, and soft tissue sarcomas.<sup>1</sup> Therefore, FASN has been emerged as an attractive therapeutic target for cancer drug discovery and development efforts.<sup>2-10</sup>

We initiated efforts to identify a novel and potent inhibitor of FASN as a potential cancer therapeutic. A high throughput screen of our compound collection was conducted against full length human FASN recombinant enzyme. In this assay, the production of coenzyme A was measured by the formation of a fluorescent CPM-CoA conjugate from the non-fluorescent reagent 7-diethylamino-3-(4'-maleimidyl-phenyl)-4-methylcoumarin (CPM). Substituted piperazines, such as the racemic compound **1**, were discovered as active FASN inhibitors ( $IC_{50} = 1.14 \mu M$ ) with drug-like properties (LE = 0.29, LipE = 4.0) suitable for follow-up (Figure 1). Further biochemical characterization suggested

compound **1** was a selective inhibitor of the ketoreductase (KR) domain of FASN (see Supplementary Material).<sup>6,11,12</sup> Synthesis and screening of the individual enantiomers of **1** identified the (*R*)-isomer (**2**) as the more potent isomer ( $IC_{50} = 1.1 \mu M$ ) with the corresponding (*S*)-isomer (**3**) showing significantly less activity ( $IC_{50} > 50 \mu M$ ). Compound **2** also had robust microsomal stability when screened in mice (100% remaining after 30-minute incubation), providing an excellent starting point for compound optimization.



**Figure 1.** Structure and activity of initial HTS hit

With the aryl acyl group at *N*4 and the polar alkyl acyl group at *N*1, these compounds were amenable to further optimization by taking advantage of Suzuki cross-couplings and subsequent amide-forming reactions. In the absence of any structural information at the outset, a ligand-based compound design approach was undertaken. Initial efforts were focused on two fronts: (1) varying the “left-hand side” (LHS) (as drawn) of the molecule while maintaining the local environment provided by the carbonyl and THF-oxygens and (2) optimizing the biaryl group on the “right-hand side” (RHS) of the molecule.

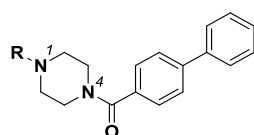
\* Corresponding author. Tel.: +1-857-209-2357; e-mail: mmartin@formatherapeutics.com

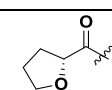
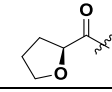
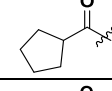
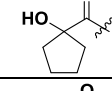
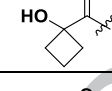
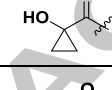
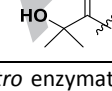
† Current Address: KSQ Therapeutics, 610 Main Street, Cambridge, MA 02139, USA

‡ Current Address: Foghorn Therapeutics, 100 Binney Street, Suite 610, Cambridge, MA 02142, USA

Table 1 summarizes our exploration of the *N1* amide. We sought to identify alternative groups that could maintain the key interactions while removing the stereogenic center. A variety of cycloalkyl systems were explored, with a distinct preference for small rings. The importance of the oxygen was confirmed, as removal resulted in almost complete loss of activity (e.g. **4**). We next explored the possibility of moving the oxygen out of the ring. Hydroxycyclopentyl analog **5** showed no significant activity ( $IC_{50} > 50 \mu M$ ), whereas hydroxycyclobutyl analog **6** ( $IC_{50} = 1.8 \mu M$ ) was equipotent with the original THF analog **2**. Hydroxycyclopropyl analog **7** showed the most promise with improvements in both potency ( $IC_{50} = 350 \text{ nM}$ ) and drug-like properties (LipE 5.3 vs 4.3 for **2**) while maintaining excellent microsomal stability. Finally, we explored opening the cycloalkyl ring (e.g. **8**); however, this change also resulted in a large loss in potency, showing the importance of the cyclopropyl ring. The combination of promising potency and drug-like properties, as well as the removal of the stereogenic center (thus avoiding any possibilities of epimerization or scrambling of stereochemistry in subsequent steps), made the hydroxycyclopropyl group a desirable option, and this group was utilized in subsequent analogs.

**Table 1.** Exploration of the *N1* Amide



R	FASN <sup>a</sup> IC <sub>50</sub> (μM)	MLM <sup>b</sup> (% 30 min)	LipE <sup>c</sup>
	1.1	100	4.3
	50	65	2.6
	50		1.2
	50		2.2
	1.8	85	4.0
	0.35	95	5.3
	35	99	2.7

<sup>a</sup>*In vitro* enzymatic potency was measured using a CPM assay with full-length recombinant human FASN enzyme. Reported as mean of at least two separate assay runs. <sup>b</sup>Mouse liver microsome stability expressed as percent remaining after 30-minute incubation. <sup>c</sup>Lipophilic efficiency =  $pIC_{50}(\text{FASN}) - \text{clogP}$ .

Our attention then turned to optimization of the biaryl right hand side of the molecule. Initial efforts focused on substituting the second aryl ring to alter the electronics. As shown in Table 2, the incorporation of electron-withdrawing groups (e.g. **9-11**) afforded modest increases in potency with little impact on other properties of the molecule. In contrast, the addition of electron donating groups, such as in **12**, exhibited decreased potency. We also examined the impact of heterocyclic substituents, and a

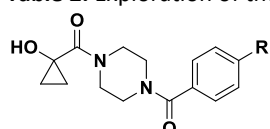
variety of 6,5- and 6,6-heteroaromatic ring-containing compounds were synthesized. As exemplified by indole analogs **13** and **14**, pyrazole **15**, benzothiazole **16**, as well as isoquinoline **18** and quinolines **19** and **20**, the introduction of polarity resulted in as much as a 10-fold improvement in potency in the biochemical assay, as well as improved properties (LipE ~ 6).

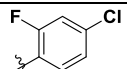
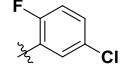
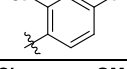
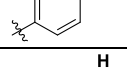
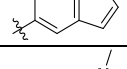
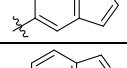
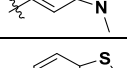
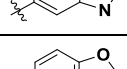
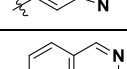
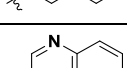
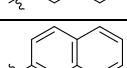
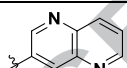
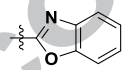
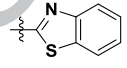
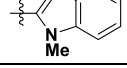
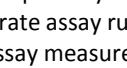
In addition to the enzymatic assay, the cellular activities of the compounds were also measured by two cell assays. In the <sup>14</sup>C-acetate incorporation assay, BT474 human breast cancer cells converted <sup>14</sup>C-acetate to <sup>14</sup>C-acetyl-CoA, which was subsequently assembled into newly synthesized radiolabeled palmitate by cellular FASN enzyme. Therefore, this assay measured the ability of FASN inhibitors to block FASN activity in a cellular context. In the second cellular assay, the proliferation of PC3 human prostate cancer cells were maintained in growth media supplemented with 10% lipid-reduced serum (LRS) in the presence of FASN inhibitor. Under LRS condition, PC3 growth has been shown to be dependent on DNL. Hence, this assay monitored functional consequence of FASN inhibition on cancer cells. As shown in Table 2, improvements in enzyme potency translated into improved cellular activity.

Based on its promising drug-like properties (LipE 6.4) and good *in vitro* ADME properties, **18** was studied in a mouse oral PK study. Unfortunately, the compound showed very little oral exposure ( $AUC_{0-8h} = 0.1 \mu M^*h$ ) after a 5 mg/kg oral dose in mice with clearance much greater than would be expected from the moderate metabolic stability observed for the compound in mouse liver microsomes.

Low oral exposures were found in several other compounds possessing similar nitrogen-containing heterocycles, such as indole **13**, benzothiazole **16**, and quinoline **19** (data not shown). One factor in this low exposure was hypothesized to be metabolism derived from aldehyde oxidase (AO), a cytosolic enzyme expressed primarily in the liver that can hydroxylate adjacent to an aromatic nitrogen.<sup>13,14</sup> To test this theory, attention was turned to the less potent phenyl analog **9** (FASN  $IC_{50} = 110 \text{ nM}$ ), featuring a di-substituted aromatic ring instead of a nitrogen-containing heterocycle. When dosed orally in mice at 5 mg/kg, **9** exhibited reasonable drug levels ( $AUC_{0-8h} = 47.6 \mu M^*h$ ). To further understand this issue, several compounds were also screened in mouse hepatocytes as well as mouse S9 fraction (a liver fraction containing microsomal and cytosolic enzymes, including AO, capable of phase 1 and 2 metabolism) to determine if a better *in vitro* to *in vivo* correlation could be identified (see Supplementary Data). Indeed, these measures did correlate much better with *in vivo* results, further supporting the hypothesis. At this stage, it was unclear if AO would be relevant in the human system, and therefore removing this liability became an area of focus.

Several compounds containing bicyclic heteroaromatic rings were then synthesized, each lacking an oxidizable CH bond adjacent to the nitrogen of the heterocycle (e.g. **22-24**). Among these, benzoxazole analog **22** was a compound with excellent potency (FASN  $IC_{50} = 50 \text{ nM}$ , PC3 proliferation  $IC_{50} = 15 \text{ nM}$ , BT474 <sup>14</sup>C incorporation  $IC_{50} = 100 \text{ nM}$ ), low intrinsic clearance ( $\sim 7 \mu L/\text{min}/\text{mg}$  in human and mouse microsomes), and overall excellent drug-like properties (LipE 5.9). When dosed at 5 mg/kg PO in mice, this compound provided excellent oral exposure ( $AUC_{0-8h} = 28.7 \mu M^*h$ ). Unfortunately, this compound was not well tolerated, with an MTD of less than 5 mg/kg in mice (single dose).

**Table 2.** Exploration of the Aryl substituent


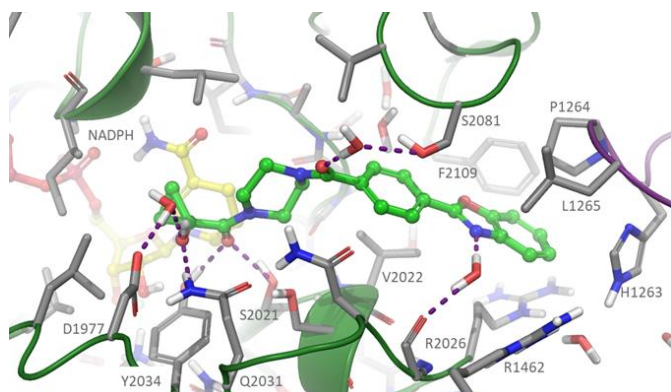
	R	FASN <sup>a</sup> IC <sub>50</sub> (μM)	PC3 <sup>b</sup> IC <sub>50</sub> (μM)	<sup>14</sup> C BT474 <sup>c</sup> IC <sub>50</sub> (μM)	MLM <sup>d</sup> (% 30 min)	Solubility <sup>e</sup> (μM)	clogP <sup>f</sup>	LipE <sup>g</sup>
9		0.11	0.146	0.336	92	33	2.0	5.0
10		0.11	0.138	0.158	66	43	2.1	4.9
11		0.31		4.96	69	67	1.7	4.8
12		3.1					1.7	3.8
13		0.016	0.004	0.018	55	60	1.5	6.3
14		0.012		0.019	81	3	1.9	6.0
15		0.026	0.012		89	79	1.2	6.4
16		0.032	0.017	0.011	88	95	2.0	5.9
17		0.142	0.142	0.257	60	92	1.2	4.9
18		0.013	0.013	0.011	45	77	1.5	6.4
19		0.010		0.012	86	82	1.5	6.5
20		0.032	0.002	0.101	79	71	1.6	5.9
21		>5		>125	89	95	0.5	4.8
22		0.054	0.015	0.101	109	83	1.3	6.0
23		0.057	0.214	0.067	84	18	1.8	5.4
24		0.033	0.025	0.070	20	0.3	1.9	4.8

<sup>a</sup>*In vitro* enzymatic potency was measured using a CPM assay with full-length recombinant human FASN enzyme. Reported as mean of at least two separate assay runs. <sup>b</sup>Anti-proliferative activity assessed in PC3 cells. Reported as mean of at least two separate assay runs. <sup>c</sup>The <sup>14</sup>C BT474 assay measured the potency of FASN inhibitors in blocking FASN activity as measured in BT474 cells. Reported as mean of at least two separate assay runs. <sup>d</sup>Mouse liver microsomes stability expressed as percent remaining after 30-minute incubation. <sup>e</sup>Kinetic solubility at pH=7.4. <sup>f</sup>Calculated logP value. <sup>g</sup>Lipophilic efficiency = pIC<sub>50</sub> (FASN) – clogP.

To verify the binding mode and potentially aid in optimization of this lead series, an X-ray crystal structure of **22** bound to a ΨME-ΨKR-KR tridomain FASN construct was solved to 2.26 Å resolution (Figure 2). The compound binds to the active site of the KR domain near the interface with the ΨKR domain. A network of key hydrogen bond interactions forms between the hydroxyl and

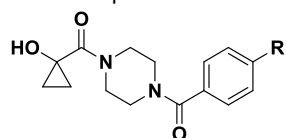
carbonyl of the hydroxycyclopropylamide and the KR domain active site residues (Ser2021, Gln2031, Tyr2034). A pi interaction is also observed between the cyclopropyl group and the nicotinamide moiety of the NADPH cofactor, confirming the importance of the cyclopropyl ring. The angle formed by the amide bond between the piperazine and the phenyl places the phenyl and

benzoxazole ring system in a narrow hydrophobic channel. The benzoxazole fills a flexible pocket at the interface of the KR and ΨKR domains. The pocket is lined with a mixture of rigid hydrophobic residues (Phe2019, Pro1264, Leu1265, Val2022) and flexible basic residues (His1263, Arg1462, Arg2026). The residues present in this pocket explain the SAR preference for heteroaromatic rings that could interact both hydrophobically and through hydrogen bonding to the basic residues. The benzoxazole in **22** fulfills these interactions including a through water interaction to Gly2027.



**Figure 2.** Co-crystal structure of **22** (2.26 Å) bound to ΨME-ΨKR tridomain FASN construct (PDB code: 6NNA)

**Table 3.** Optimization of the Benzoxazole substituent



R	FASN <sup>a</sup> IC <sub>50</sub> (μM)	PC3 <sup>b</sup> IC <sub>50</sub> (μM)	<sup>14</sup> C BT474 <sup>c</sup> IC <sub>50</sub> (μM)	MV-411 <sup>d</sup> IC <sub>50</sub> (μM)	MLM <sup>e</sup> (% 30 min)	Solubility <sup>f</sup> (μM)	clogP <sup>g</sup>	LipE <sup>h</sup>
	0.069	0.049	0.136		85	6	1.8	5.4
	0.097	0.029	0.104		92	7	1.8	5.3
	0.192	0.052	0.061		93	30	1.3	5.4
	0.213	0.047	0.090	0.026	100	39	1.3	5.4

<sup>a</sup>*In vitro* enzymatic potency was measured using a CPM assay with full-length recombinant human FASN enzyme. Reported as mean of at least two separate assay runs. <sup>b</sup>Anti-proliferative activity assessed in PC3 cells. Reported as mean of at least two separate assay runs. <sup>c</sup>The <sup>14</sup>C BT474 assay measured the potency of FASN inhibitors in blocking FASN activity as measured in BT474 cells. Reported as mean of at least two separate assay runs. <sup>d</sup>Anti-proliferative activity assessed in MV-411 cells. Reported as mean of at least two separate assay runs. <sup>e</sup>Mouse liver microsome stability expressed as percent remaining after 30-minute incubation. <sup>f</sup>Kinetic solubility at pH=7.4. <sup>g</sup>Calculated logP value. <sup>h</sup>Lipophilic efficiency = pIC<sub>50</sub> (FASN) – clogP.

**Table 4.** Pharmacokinetic Profile of **FT113** after oral dosing

Species	Dose (mg/kg)	<i>t</i> <sub>max</sub> (h)	<i>C</i> <sub>max</sub> (μM)	AUC <sub>0-8h</sub> (μM*h)	Bioavailability (%)
Mouse <sup>a</sup>	5	2	8.4	46	95
Species	Dose (mg/kg)	<i>t</i> <sub>max</sub> (h)	<i>C</i> <sub>max</sub> (μM)	AUC <sub>0-24h</sub> (μM*h)	Bioavailability (%)
Rat <sup>b</sup>	5	3	33	440	84

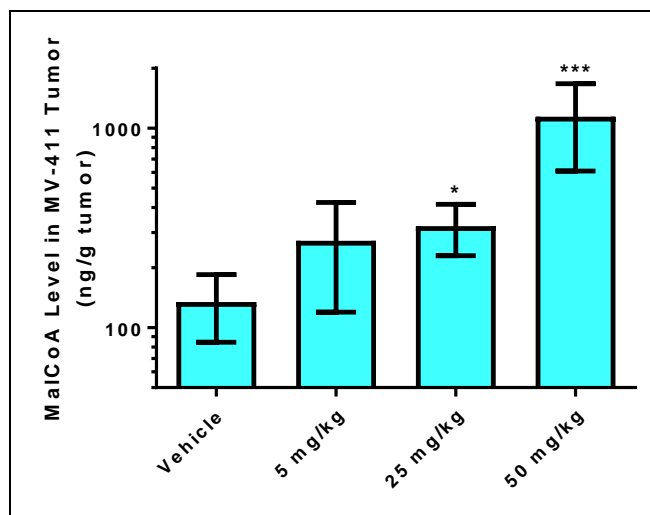
The initial promising potency and PK properties of **22**, coupled with the structural insights obtained from the crystal structure, guided further optimization (Table 3). We sought to mitigate the potential toxicity of the benzoxazole series by blocking the sites para to the anilino nitrogen and phenolic oxygen, areas known to form reactive metabolites.<sup>15</sup> Thus, 5- and 6-substituted benzoxazoles were examined (e.g. **25-27**, **FT113**). Introduction of chloro- and fluoro-substitution had minimal effect on potency and the overall physicochemical properties. However, some decrease in solubility was observed for the chloro analogs. Fluoro analogs **27** and **FT113** were ultimately identified as the compounds with the best balance of potency and physicochemical properties, and both were advanced to *in vivo* studies.

The pharmacokinetic properties of fluoro-benzoxazoles **27** and **FT113** were assessed in mice. Upon oral dosing at 5 mg/kg in female Balb/c nude mice, a stark contrast was observed. 5-Fluorobenzoxazole analog **27** was not tolerated, displaying acute toxicity after a single 5 mg/kg dose. In contrast, 6-fluorobenzoxazole **FT113** showed no acute toxicity and provided excellent exposure when dosed orally at 5 mg/kg (AUC<sub>0-8h</sub> = 46 μM\*h, see Table 4). These findings suggest blocking of the 6-position is important to the prevention of potentially reactive metabolites. The PK properties of **FT113** were further profiled in rats. Upon oral dosing at 5 mg/kg in male Sprague-Dawley rats, **FT113** displayed excellent exposure (AUC<sub>0-24h</sub> = 440 μM\*h, see Table 4) and bioavailability (84%).

<sup>a</sup>Dosed p.o. in female Balb/c nude mice (*n*=6). Dosing formulation: PEG400/Ethanol (9:1). <sup>b</sup>Dosed p.o. in male Sprague Dawley rats (*n*=3). Dosing formulation: PEG400/Ethanol (9:1).

We investigated the *in vivo* potency of compound **FT113** in mouse models subcutaneously xenografted with human cancer cell line MV-411. When the tumor size reached 130-140 mm<sup>3</sup>, the xenografted mice were randomized based on tumor size into four groups (N=4 mice/group) and received vehicle (9:1 (v/v) PEG400/ethanol), or 5, 25, or 50 mg/kg of **FT113** twice daily for

16 days. At 4 hour post last dose, the mice were euthanized and the malonyl-CoA (FASN substrate) in xenograft tumor samples was measured by LC-MS. **FT113** treatment showed dose-dependent increase of malonyl-CoA concentration in tumors in treated vs. vehicle groups, indicating FASN inhibition in the tumor tissue (Figure 3). In addition, treatment with 25 and 50 mg/kg of **FT113** achieved 32 % and 50% tumor growth inhibition, respectively, vs. the vehicle group after 16-day treatment (data not shown), suggesting that FASN inhibitors could hold promise for activity against cancer and, as such, merit further study.



**Figure 3.** MalonylCoA levels in MV-411 mouse xenograft model. Athymic nude mice ( $n=4$ ) were treated b.i.d. with **FT113** for 16 days at the indicated doses. Tumors were collected 4 h post last dose and MalonylCoA levels were measured by LC-MS. Error bars represent +/- SEM. P values of \* indicates  $p < 0.05$ ; \*\*\* indicates  $p < 0.0005$ , as determined by one-way ANOVA vs. vehicle control.

**FT113** was synthesized from readily available starting materials according to the concise route illustrated in Scheme 1. Condensation of methyl 4-(chlorocarbonyl)benzoate (**28**) with 2-amino-5-fluorophenol (**29**) in the presence of methane sulfonic acid provided 2-arylbenzoxazole **30** in 66% yield. Saponification with lithium hydroxide yielded carboxylic acid **31**, which was reacted with *tert*-butyl piperazine-1-carboxylate under standard amide coupling conditions to afford piperazine amide **32** in 56% overall yield. Removal of the Boc-protecting group with hydrochloric acid provided piperazine **33** as its hydrochloride salt in near quantitative yield. Subsequent treatment of **33** with 1-hydroxycyclopropane-1-carboxylic acid under amide coupling conditions afforded the desired product **FT113** in 47% yield.

In summary, we have described the discovery of a novel series of piperazines as potent FASN inhibitors. Systematic SAR exploration allowed for the rapid identification of the optimal groups necessary for efficient binding. This led to the discovery of compound **FT113**, which had the best balance of potency and *in vitro* and *in vivo* PK/PD properties, enabling its use as a tool to develop POC in models of DNL driven disease. Upon daily dosing, compound **FT113** demonstrates significant increases in malonylCoA concentrations as well as tumor growth inhibition.

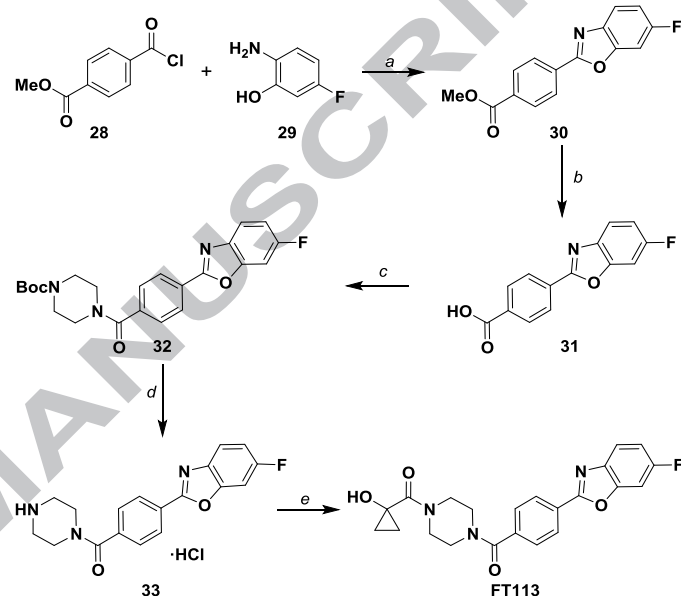
## Acknowledgments

We thank Hien Diep for *in vitro* ADME support, Scot Mente for statistical analysis and helpful discussions, and Mark Tebbe and James Loch for contributions to compound design and

synthesis. We also thank Viva Biotech (Shanghai) Ltd. for the FASN co-crystal structure with compound **22**.

## Supplementary Material

Supplementary material associated with this article (including details of the *in vitro* FASN enzyme and cellular assays; the MV-411 xenograft mouse model; FASN protein expression, purification, crystallization, and X-ray structure solution; as well as experimental procedures for the synthesis of compound **FT113**) can be found in the online version.

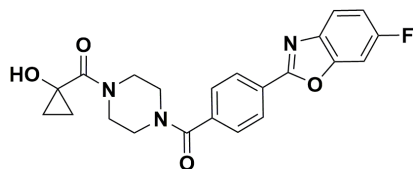


**Scheme 1.** Synthesis of 2-arylisoindoline-4-carboxamides. Reagents and conditions: (a) methanesulfonic acid, 1,4-dioxane, 100 °C, 24 h, 66%; (b) LiOH, 1,4-dioxane, H<sub>2</sub>O, rt, 5 h, 100%; (c) *tert*-butylpiperazine-1-carboxylate, EDC-HCl, HOBT, NMM, DMF, 4 h, 56 %; (d) HCl, Et<sub>2</sub>O, 18 h, 98%; (e) 1-hydroxycyclopropane-1-carboxylic acid, EDC-HCl, HOBT, NaOH EtOH, 24 h, 47 %.

## References and notes

- Menendez JA, Lupu R. Fatty acid synthase and the lipogenic phenotype in cancer pathogenesis. *Nat Rev Cancer*. 2007;7(10):763-777. doi:10.1038/nrc2222
- Kridel SJ, Lowther WT, Pemble CW. Fatty acid synthase inhibitors: new directions for oncology. *Expert Opin Investig Drugs*. 2007;16(11):1817-1829. doi:10.1517/13543784.16.11.1817
- Kridel SJ. Orlistat Is a Novel Inhibitor of Fatty Acid Synthase with Antitumor Activity. *Cancer Res*. 2004;64(6):2070-2075. doi:10.1158/0008-5472.CAN-03-3645
- Vázquez MJ, Leavens W, Liu R, et al. Discovery of GSK837149A, an inhibitor of human fatty acid synthase targeting the  $\beta$ -ketoacyl reductase reaction. *FEBS J*. 2008;275(7):1556-1567. doi:10.1111/j.1742-4658.2008.06314.x
- Oslob JD, Johnson RJ, Cai H, et al. Imidazopyridine-Based Fatty Acid Synthase Inhibitors That Show Anti-HCV Activity and *in Vivo* Target Modulation. *ACS Med Chem Lett*. 2013;4(1):113-117. doi:10.1021/ml300335r
- Hardwicke MA, Rendina AR, Williams SP, et al. A human fatty acid synthase inhibitor binds  $\beta$ -ketoacyl reductase in the keto-substrate site. *Nat Chem Biol*. 2014;10(9):774-779. doi:10.1038/nchembio.1603
- Ventura R, Mordec K, Waszczuk J, et al. Inhibition of *de novo* Palmitate Synthesis by Fatty Acid Synthase Induces Apoptosis in Tumor Cells by Remodeling Cell Membranes, Inhibiting Signaling Pathways, and Reprogramming Gene Expression. *EBioMedicine*. 2015;2(8):808-824. doi:10.1016/j.ebiom.2015.06.020

8. Angeles TS, Hudkins RL. Recent advances in targeting the fatty acid biosynthetic pathway using fatty acid synthase inhibitors. *Expert Opin Drug Discov.* 2016;11(12):1187-1199. doi:10.1080/17460441.2016.1245286
9. Buckley D, Duke G, Heuer TS, et al. Fatty acid synthase - Modern tumor cell biology insights into a classical oncology target. *Pharmacol Ther.* February 2017. doi:10.1016/j.pharmthera.2017.02.021
10. Lu T, Schubert C, Cummings MD, et al. Design and synthesis of a series of bioavailable fatty acid synthase (FASN) KR domain inhibitors for cancer therapy. *Bioorg Med Chem Lett.* 2018;28(12):2159-2164. doi:10.1016/j.bmcl.2018.05.014
11. Maier T, Leibundgut M, Ban N. The Crystal Structure of a Mammalian Fatty Acid Synthase. *Science.* 2008;321(5894):1315-1322. doi:10.1126/science.1161269
12. Weissman KJ. Taking a Closer Look at Fatty Acid Biosynthesis. *ChemBioChem.* 2008;9(18):2929-2931. doi:10.1002/cbic.200800671
13. Pryde DC, Dalvie D, Hu Q, Jones P, Obach RS, Tran T-D. Aldehyde oxidase: an enzyme of emerging importance in drug discovery. *J Med Chem.* 2010;53(24):8441-8460. doi:10.1021/jm100888d
14. Pryde DC, Tran T-D, Jones P, et al. Medicinal chemistry approaches to avoid aldehyde oxidase metabolism. *Bioorg Med Chem Lett.* 2012;22(8):2856-2860. doi:10.1016/j.bmcl.2012.02.069
15. Plampin JN, Cain CK. Synthesis of Metabolic Products of Benzoxazoles 1. *J Med Chem.* 1963;6(3):247-248. doi:10.1021/jm00339a006

**FT113**FASN IC<sub>50</sub> = 213 nMMV411 cell IC<sub>50</sub> = 26 nM

%F(mouse) = 95%

ACCEPTED MANUSCRIPT

## Discovery and Optimization of Novel Piperazines as Potent Inhibitors of Fatty Acid Synthase (FASN)

Matthew W. Martin,<sup>a,\*</sup> David R. Lancia, Jr.,<sup>a</sup> Hongbin Li,<sup>b</sup> Shawn E. R. Schiller,<sup>a</sup> Angela V. Toms,<sup>a</sup> Zhongguo Wang,<sup>a</sup> Kenneth W. Bair,<sup>a</sup> Jennifer Castro,<sup>a</sup> Shawn Fessler,<sup>a</sup> Deepali Gotur,<sup>a</sup> Stephen E. Hubbs,<sup>b</sup> Goss S. Kauffman,<sup>b</sup> Mark Kershaw,<sup>b</sup> George P. Luke,<sup>b</sup> Crystal McKinnon,<sup>a</sup> Lili Yao,<sup>b</sup> Wei Lu,<sup>a</sup> and David S. Millan<sup>a</sup>

<sup>a</sup>FORMA Therapeutics, 500 Arsenal Street, Suite 100, Watertown, MA 02472, USA

<sup>b</sup>FORMA Therapeutics, 35 Northeast Industrial Road, Branford, CT 06405, USA

### Highlights

- Identified novel and potent inhibitors of FASN KR domain
- Synthesis and structure activity relationships of compounds are reported
- **FT113** displays excellent cellular activity and pharmacokinetic properties
- **FT113** is a valuable tool to develop POC models of DNL driven disease